

Research on Morphology and Growth Mechanism of Xonotlite Crystal

F Liu^{1,2,3}, S Chen^{1,3}, Q Lin^{1,2}, X D Wang² and J X Cao^{1,2,3,*}

¹ School of Chemistry and Chemical Engineering, Guizhou University, Guiyang, Guizhou 550025, PR China

² Key Laboratory of Green Chemical and Clean Energy Technology, Guiyang, Guizhou 550025, PR China

³ Key Laboratory of Efficient Utilization of Mineral and Green Chemical Technology, Guiyang, Guizhou 550025, PR China

* jxcao@gzu.edu.cn

Abstract. The xonotlite crystals were synthesized via the hydrothermal synthesis manner from CaO and SiO₂ as the raw materials with their Si/Ca molar ratio of 1.0. The morphologies and their growth mechanisms of xonotlite crystal were explored by taking the various siliceous sources into account in this paper. These products were characterized by XRD and SEM techniques to investigate their crystalline phase and morphology. The results indicated that siliceous material had little influence on the crystalline phases of xonotlite crystals but posed a great impact on their morphologies. Based on the various morphologies characteristics of the products, the growth mechanism for the morphologies of spherical particles and fibers were further revealed according with the in situ transformation mechanism and dissolution-precipitation mechanism respectively.

1. Introduction

Xonotlite has been widely utilized in the fields of thermal insulation, architecture and so on, for its distinct physical and chemical properties, such as thermal stability, biological activity and environmental friendliness[1-5]. Therefore, the preparation of xonotlite crystals has become one of the research hotspots in recent years. In general, the xonotlite products used in industry were fabricated using dynamic hydrothermal synthesis method from CaO and SiO₂ as the raw materials with their Si/Ca molar ratio of 1.0[6-9]. The previous researches revealed that raw materials posed a great impact on the growth of xonotlite crystals[10-14]. Due to those factors such as raw materials and unclear growth mechanism of xonotlite crystals, the morphologies of the products were quite different and uncontrollable. Accordingly, based on the previous studies in our group[15-16], the morphologies and their growth mechanism of xonotlite crystals were particularly explored by taking H₂SiO₃ and K₂SiO₃ as siliceous materials respectively into account, aiming to make the morphologies of the xonotlite crystals be controllable.

2. Materials and methods

The xonotlite crystals were synthesized via the hydrothermal synthesis method.

H₂SiO₃ and K₂SiO₃ solutions were used as siliceous materials respectively. Ca(OH)₂ suspension as calcareous material was prepared by mixing CaCl₂ with KOH 100g L⁻¹ at the molar ratio of 1:2. The



calcareous material, distilled water, and siliceous material (H_2SiO_3 or K_2SiO_3 solution) were homogeneously mixed, and then the mixture was transferred into a reaction chamber with a stirrer at a heating rate of $1.5\text{ }^\circ\text{C}\cdot\text{min}^{-1}$ and a stirring rate of 200 rpm. The hydrothermal treatment proceeded under the following conditions: the Ca/Si molar ratio of 1.0, the reaction temperature of $225\text{ }^\circ\text{C}$, the reaction time of 15 h. After the hydrothermal treatment, the suspensions were filtrated and washed three times by distilled water. The resultant powders were dried at $75\text{ }^\circ\text{C}$ for 12 h. Technological flow diagram of hydrothermally synthesizing xonotlite products was shown in figure 1.

The crystalline phase composition and microstructure characteristics of the samples were characterized by X-ray diffraction (XRD, Model D/max-2200, Japan). A scanning electron microscope (SEM, Model JSM-6490LV, operating at 25 KV, Japan) was used to observe the morphology of xonotlite crystals.

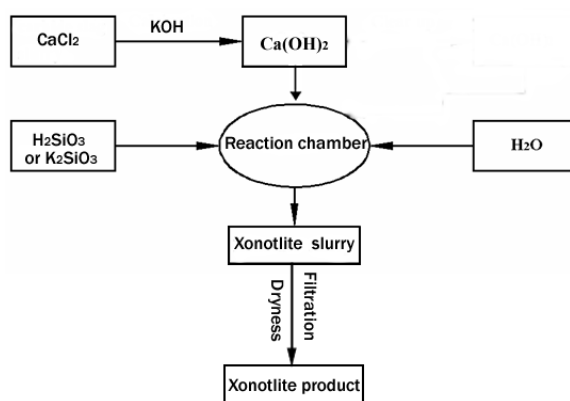


Figure 1. Technological flow diagram of hydrothermally synthesizing xonotlite products

3. Results and discussion

Figure 2 shows the XRD patterns of the products synthesized hydrothermally at $225\text{ }^\circ\text{C}$ for 15 h from various siliceous materials. Clearly, the main crystalline phases prepared by hydrothermal synthesis method with various siliceous materials were xonotlite (corresponding to $\text{Ca}_6\text{Si}_6\text{O}_{17}(\text{OH})_2$, standard JCPDS card No. 23-0125).

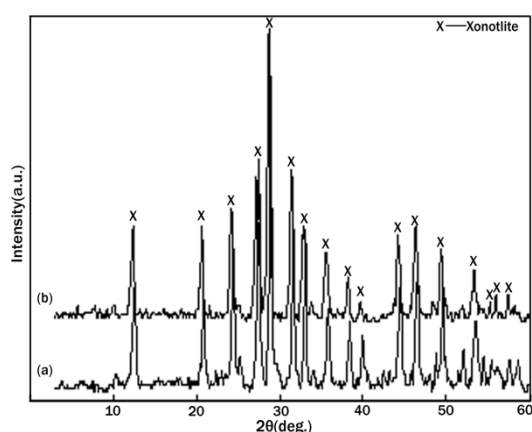


Figure 2. X-ray diffraction patterns of the products hydrothermally synthesized from various siliceous materials

(a) H_2SiO_3 as siliceous material; (b) K_2SiO_3 as siliceous material

From the analysis result of XRD patterns, the existence of a series of strong diffraction peaks showed that the xonotlite crystal from K_2SiO_3 solution as siliceous material was well-crystallized and almost no impurity. Meanwhile, the intensity of diffraction peak was also strong when using H_2SiO_3 solution as siliceous material, indicating that the pure xonotlite crystalline phase was completely obtained in the synthesis system.

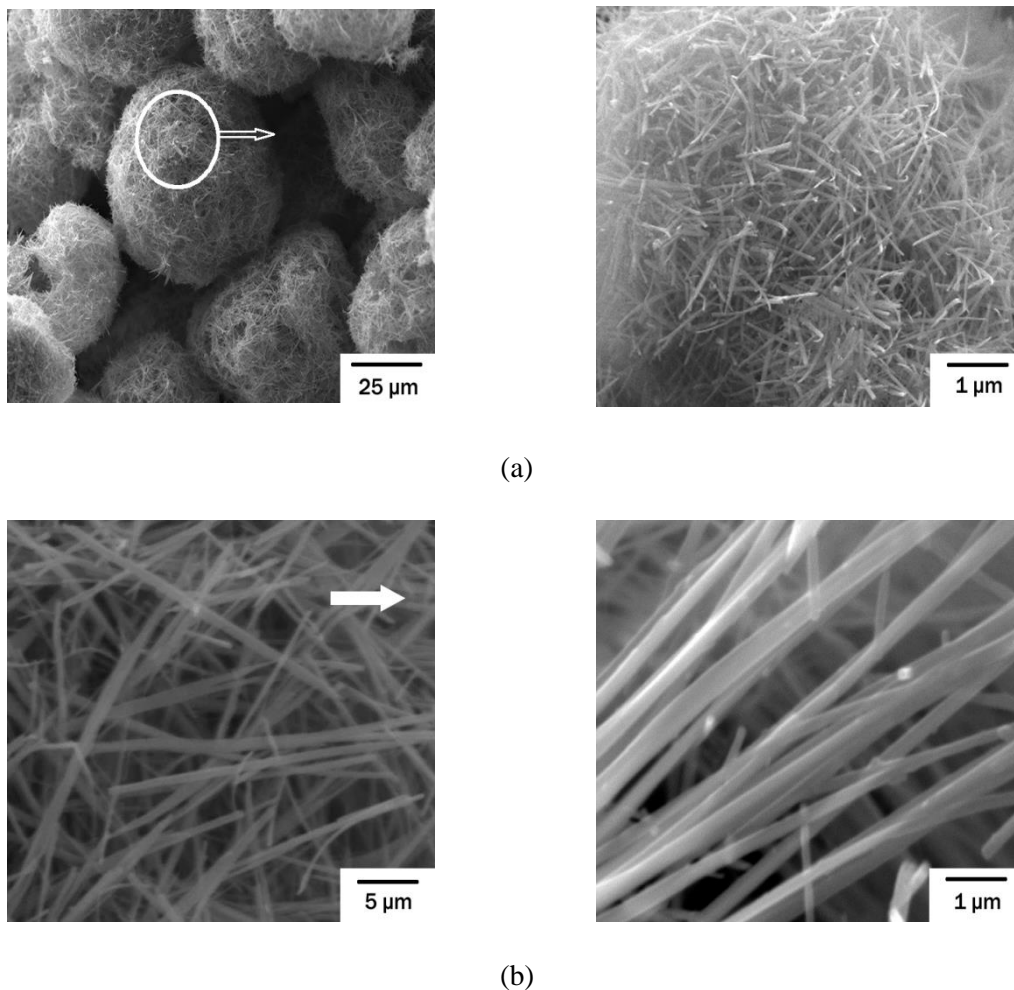


Figure 3. SEM images of the products hydrothermally synthesized from various siliceous materials

(a) H_2SiO_3 as siliceous material; (b) K_2SiO_3 as siliceous material

Figure 3 displays the SEM images of the products synthesized from various siliceous materials. Using H_2SiO_3 as siliceous material, the products obtained by hydrothermal synthesis were spherical particles with diameters of 20-50 μm , which were formed by a large number of short xonotlite fibers disordered intertwined. While using K_2SiO_3 as the siliceous material, the morphology of xonotlite crystal was typical fiber and its aspect ratio was approximately 50-100, with the length of 20-40 μm and the diameter of approximately 400 nm.

The dissociation constant values of H_2SiO_3 were extremely low ($K_{a(1)}=2.5\times 10^{-10}$, $K_{a(2)}=1.6\times 10^{-12}$, $K_{a(3)}=1.0\times 10^{-12}$), then H_2SiO_3 was extremely difficult to dissolve in the water at room temperature when used H_2SiO_3 as siliceous material. The growth mechanism of xonotlite spherical particles synthesized by the hydrothermal synthesis method could be explained by in situ transformation mechanism. It means that these reactions took place on the surface of precursor particles without dissolution to obtain crystal particles of products. The schematic diagram of in situ transformation mechanism was shown in figure 4.

In the process of hydrothermal synthesis for xonotlite crystals, the solubility of the siliceous precursor increased with the elevation of the reaction temperature and pH value, so that the siliceous precursor had been partially ionized into HSiO_3^- and SiO_3^{2-} ions, which initially reacted with Ca^{2+} and OH^- ions introduced from Ca(OH)_2 ionization to synthesize poorly crystalline C-S-H (hydrated

calcium silicate) gels. Then the C-S-H gels wrapped on the surface of spherical aggregates of siliceous material to form spherical colloidal particles. At this time, the remaining Ca^{2+} and OH^- spread on the thin layers of spherical aggregate to participate in reaction until siliceous material completely depleted. As a result, the spherical colloidal particles turned into spherical gel particles with distinct hollow structure. As extension of the reaction time, a series of reactions from C-S-H into the acicular xonotlite crystals took place on the surface of the hollow spherical gel.

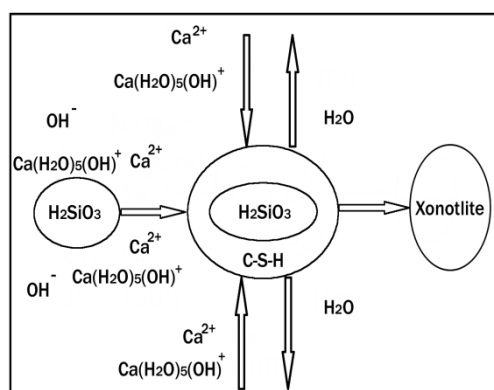


Figure 4. The schematic diagram of in situ transformation mechanism

The aforementioned growth mechanism of xonotlite spherical aggregates conformed to the in situ transformation mechanism that the growth of the xonotlite crystal existed on the surface of the undissolved siliceous precursor particles. After a period of time, the siliceous materials surrounded by a special thin layers of C-S-H gel gradually dissolved, and ultimately turned into the spherical particles with distinct hollow structure.

Using K_2SiO_3 as siliceous material, the growth mechanism of xonotlite fibers synthesized via the hydrothermal synthesis method could be interpreted by the dissolution-precipitation mechanism. It means that the precursor expeditiously dissolved to form hydrated ions or other complex ions, resulting in the formation of xonotlite crystal nucleus through transition phase. Meanwhile, remaining precursors provided ions for the growth of crystal nucleus or the formation of new crystal nucleus.

The dissolution-precipitation mechanism for the growth of xonotlite fibers involved several steps. At room temperature, $\text{Ca}(\text{OH})_2$ exhibits obviously solubility, and the $\text{Ca}(\text{H}_2\text{O})_5(\text{OH})^+$ hydrated ions and SiO_3^{2-} anionic groups are considerably formed by the dissolution of $\text{Ca}(\text{OH})_2$ in aqueous solution. The collinear reactions, taking place between $\text{Ca}(\text{H}_2\text{O})_5(\text{OH})^+$ hydrated ions and SiO_3^{2-} anionic groups, formed the Ca-O bonds which had been squeezed and finally developed into CaO_2 chips with the characteristics of tobermorite. Both sides of the CaO_2 chips combined with $[\text{SiO}_4]$ triple chains and OH^- ions respectively to synthesize semi-crystalline C-S-H gels. With the reaction time increasing, C-S-H gels crystallized into C-S-H(II) firstly, then generated into C-S-H(II), which was similar to the tobermorite. But C-S-H(II) was unstable at the reaction temperature (above 220°C), resulting in the interlayer water molecules of C-S-H(II) strongly rotated and activated to the extent of transiting to adjacent lattices.

The gap between the CaO_2 chips and $[\text{SiO}_4]$ triple chains was too narrow, so the interlayer water molecules could only dissociate into OH^- ions attracting free Ca^{2+} ions. The triple chains adjacent to each other condensed into double triple chains of $[\text{Si}_6\text{O}_{17}]^{10-}$, which was paralleled to the b-axis. The Ca^{2+} ions from the chains of $[\text{Si}_6\text{O}_{17}]$ had adopted six-coordinated to form Ca-O₆ octahedrons connecting by edges, and those octahedrons had played a role of connector between dual chains. The octahedrons formed a crystal structure with double chains when the characteristics of CaO_2 chips gradually disappeared. The xonotlite crystal was mainly grown along the b-axis direction, and the growth rate of the crystal in the b-axis direction was much faster than that in other directions, ultimately leading to the formation of acicular or fibrous shape.

From the above analysis, at the initial stage, a large amount of SiO_3^{2-} ions introduced from siliceous material was an essential prerequisite to the formation of xonotlite fibers. In the experimental process of hydrothermal synthesis, the nucleation and growth of the xonotlite had generally finished during the high temperature stage. However, $\text{Ca}(\text{OH})_2$ had a unique dissolution characteristic at constant temperature, and its solubility decreased with hydrothermal temperature increasing. Thus, the solubility of $\text{Ca}(\text{OH})_2$ was extremely low at reaction temperature of 225 °C so that the rate of Ca^{2+} ions releasing into the solution was also slow and controllable, contributing to the nucleation and growth of the xonotlite fiber without the appearance of explosive nucleation section.

4. Conclusions

Siliceous material had little influence on the crystalline phases of xonotlite crystals but posed a great impact on their morphologies. The morphologies of xonotlite crystal via hydrothermal synthesis route were significantly determined by the various precursor states of siliceous materials. The xonotlite crystal from H_2SiO_3 and K_2SiO_3 as siliceous materials could be grown to form the various morphologies of spherical particles and fibers respectively. The growth mechanism for the morphology of spherical particles was accorded with the in situ transformation mechanism due to the reactions on the surface of the precursor particles without dissolution. The growth mechanism for the morphology of fibers was conformed to the dissolution-precipitation mechanism, and a large amount of SiO_3^{2-} ions introduced from siliceous material was an essential prerequisite to the formation for xonotlite fibers.

Acknowledgments

We gratefully acknowledge the supports of this work by the National Natural Science Foundation of China (Grant No. 21666007), Science Technology Foundation of Guizhou (Grant No. 2014-2007) and Program for “Hundred” High-level Talents in Guizhou (Grant No. 2016-5655).

References

- [1] Zou J J, Guo C B, Wei C D and Jiang Y S 2016 *Res. Chem. Intermed* **42** 519-30
- [2] Hsiang H, Chen W S and Huang W C 2016 *Mater. Struct* **49** 905-15
- [3] Liu L, Yue Y and Cao J X 2014 *Mater. Sci. Forum* **809-810** 672-5
- [4] Zhang S G, Xie H B and Li G Z 2006 *Energy-Saving. Mater* **34** 28-30
- [5] Liu F, Wang X D and Cao J X 2012 *Chin. J* **57** 3323-28
- [6] Zou J, Guo C, Wei C, Jiang Y and Li F 2016 *Mater. Chem. Phys* **172** 121-8
- [7] Hartmann A, Schulenberg D and Buhl J C 2015 *J. Mater. Sci. Technol. Chem. Eng* **3** 39-55
- [8] Liu F, Zhu B and Cao J X 2011 *Adv. Mater. Res* **148-149** 1755-8
- [9] Yang J, Zhang X, Ma H W, Wang M W and Wu H 2014 *Key Eng. Mater* **633** 7-10
- [10] Black L, Garbev K and Stumm A 2009 *Adv. Appl. Ceram* **108** 137-44
- [11] Guo X Y, Ma S H, Lü S Q, Zheng S L and Zou X 2015 *Chin. J. Nonferrous. Metals* **25** 534-44
- [12] Spudulis E, Šavareika V and Špokauskas A 2013 *Mater. Sci* **19** 190-6
- [13] Baltakys K and Prichockiene E 2010 *Mater. Sci-Poland* **28** 295-304
- [14] Bao Y W, Jiang D Y and Gong J H 2017 *Key Eng. Mater* **726** 569-75
- [15] Liu F, Wang X D and Cao J X 2013 *Int. J. Min. Met. Mater* **20** 88-93
- [16] Liu F, Zeng L K, Cao J X and Li J 2010 *J. Wuhan. Univ. Technol* **25** 295-7